

Contents lists available at [SciVerse ScienceDirect](http://www.sciencedirect.com)

Journal of Quantitative Spectroscopy & Radiative Transfer

journal homepage: www.elsevier.com/locate/jqsrt

Long-term trends of precipitable water and precipitation over the Tibetan Plateau derived from satellite and surface measurements



Dingling Zhang, Jianping Huang*, Xiaodan Guan, Bin Chen, Lei Zhang

Key Laboratory for Semi-Arid Climate Change of the Ministry of Education, College of Atmospheric Sciences, 222 Tianshui Southroad, Lanzhou University, Lanzhou 730000, China

ARTICLE INFO

Article history:

Received 8 August 2012

Received in revised form

19 November 2012

Accepted 26 November 2012

Available online 25 December 2012

Keywords:

Precipitable water

Loss of water resources

Tibetan Plateau

Satellite remote sensing

Himalayas

ABSTRACT

This study investigated the long-term trends of precipitable water and precipitation over the Tibetan Plateau using satellite and surface measurements. The results show that precipitable water in the 680–310 hPa layer of the atmosphere has increased significantly since the 1990s, with an upward trend of 6.45 cm per decade and particularly high increases in summer. However, precipitation has not shown a significantly increasing trend, and the land surface has become drier in parts of the Himalayas. The increased moisture in the atmosphere may be the result of two processes: (1) the rapid melting of glaciers and snow over the Tibetan Plateau due to enhanced regional warming and (2) a small increase in water vapor transported from low-latitude ocean sources and the Arabian Sea. Analyses of precipitation, evaporation, and the Palmer drought severity index (PDSI) indicated that the water resources on the Tibetan Plateau are decreasing and that the water storage capacity in the Himalayas may be permanently lost.

© 2012 Elsevier Ltd. All rights reserved.

1. Introduction

The Tibetan Plateau is the highest and largest plateau on Earth and includes some of the most complex terrain on the globe. After the Antarctic and Arctic, the Tibetan Plateau is also one of world's largest stores of ice, although this feature of the Tibetan Plateau receives comparatively little attention. The high altitude, geographic location, and topography of the Tibetan Plateau make it an important "Asian water tower," holding glaciers, snowpacks, lakes, and rivers. The runoff from the Tibetan Plateau feeds seven major rivers in Asia, including the Yangtze, Yellow River, Ganges, Indus, Brahmaputra, Salween, and Mekong [1–3]. These waters sustain life and agricultural and industrial water usage for nearly 40% of the world's population.

Water vapor in the atmosphere plays an important role in supplying the Asian water tower. A water vapor maximum

occurs above 500 hPa in the atmospheric columns over the Tibetan Plateau [4]. In the lower troposphere, water vapor is the main resource for precipitation in all weather systems, generating latent heating and dominating the structure of diabatic heating in the troposphere [5]. Water vapor in the atmosphere directly affects the water storage of the Tibetan Plateau. Thus, understanding changes in water vapor over the plateau is important because any changes might affect the water supplies for billions of people. In this study, we investigated the long-term trends in precipitable water over the Tibetan Plateau and presented possible explanations for the trends observed. We also studied the potential impacts of these changes.

2. Data and methodology

We used three types of data for this study: (1) satellite remote sensing data, (2) meteorological station data, and (3) reanalysis data. The satellite remote sensing dataset consisted of the following. Monthly mean cloud cover and monthly mean precipitable water for 680–310 hPa were obtained at a

* Corresponding author. Tel.: +86 931 8914282.
E-mail address: hjp@lzu.edu.cn (J. Huang).

spatial resolution of 2.5° by 2.5° from the D2 dataset of the International Satellite Cloud Climatology Project (ISCCP), which began in July 1983 [6]. The snow depth dataset was based on passive microwave satellite observations from the US National Snow and Ice Data Center (NSIDC) including observations made by the Scanning Multichannel Microwave Radiometer (SMMR) (1978–1987), Special Sensor Microwave Imager (SSM/I) (1987–2008), and the Advanced Microwave Scanning Radiometer for the Earth Observing System (AMSR-E) (2002–2010). Because the three sensors were boarded on different platforms, the data acquired by the sensors displayed a systemic inconsistency. Dai and Che improved the temporal consistency of the brightness temperature via a cross-calibration of different sensors and they retrieved the snow depth using an improved algorithm, which was specialized for the China region based on the Chang algorithm [7–9]. These data also had a spatial resolution of 2.5° by 2.5° . In addition, snow cover data for the last 12 years (2000–2011) observed by the Moderate Resolution Imaging Spectroradiometer (MODIS)/Terra were obtained from the NSIDC. Considering that the snow cover over an area is typically described by the fraction of snow-covered land, monthly composites of the snow cover fraction (SCF) in a 0.05° by 0.05° climate modeling grid (MOD10CM) were used in this study [10]. The quality of MODIS snow data over the Tibetan Plateau has been previously evaluated [11–13].

Meteorological station data for the Tibetan Plateau has been reported directly from benchmark surface weather stations and automatic weather stations since 1951. The analyzed variables include annual mean surface air temperature, annual mean surface precipitation, and daily small pan evaporation.

The reanalysis data included mean monthly surface air temperature and precipitation data from the Climate Research Unit (CRU version TS3.1) with a resolution of 0.5° by 0.5° for the period of 1901 to 2009 provided by the University of East Anglia [14]. A monthly dataset of the Palmer drought severity index (PDSI) from 1850 to 2010, derived using historical precipitation and temperature data for global land areas, was also used [15]. In addition we used the South Asia monsoon index (SAMI) from 1948 to 2010 [16]. To compare results, all the datasets consulted included the period of 1984–2009.

To study trends over the Tibetan Plateau, we first calculated regional average values for several variables over the Tibetan Plateau domain ($25\text{--}40^\circ\text{N}$, $70\text{--}105^\circ\text{E}$) as the simple arithmetic mean of all stations or grids higher than 2500 m a.s.l. In the following analyses, anomaly values from the CRU and station data were computed relative to 1961–1990; this period was chosen because it had the best coverage of CRU data, which facilitated comparisons between stations [17]. Annual temperature anomalies were also computed relative to the 1961–1990 mean. For the other datasets, anomaly values were calculated over the time series provided by the data. Finally, to detect trends, we used the following linear regression:

$$y = a + bx$$

where y denotes the variable anomaly at time x (in years), a is the intercept, and the trend b is the slope of the straight

line, which represents the rate of increase or decrease of the variable anomaly. The regression coefficients a and b were determined by a least-square fitting.

3. Analysis of results

A pool of concentrated water vapor over the Tibetan Plateau has previously been reported [4], especially at high levels. For the period 1984–2009, the trend in the spatial distribution of precipitable water at 680–310 hPa over the Tibetan Plateau was significantly different from that over surrounding areas. An increasing trend was found over nearly the entire plateau, and for most of the area this was significant at the 0.01 level. The highest positive trend occurred over the central region of the Tibetan Plateau, where the maximum increase was as much as 10 cm per decade (Fig. 1a). The farther from the center of the plateau an area was, the lower the positive trend was. Comparing different seasons, Fig. 2b shows intense increasing trends for summer (June–August) and autumn (September–November) but weak trends for spring (March–May) and winter (December–February). Although the summer trend was most pronounced, with a maximum value of 1.89 cm/decade ($p < 0.01$), the summer precipitable water in the 680–310 hPa anomaly had the largest variability, especially after 1998. Unfortunately, the exact reason for the “jump” feature during 1997–1998 is still unknown. There is not a specific event that occurred during 1997–1998 which would explain this. In a study of large-scale atmospheric moisture processes, Peixoto et al. [18] found that water vapor levels contrasted between summer and winter. This pattern was not observed in spring and autumn, when instead the pattern resembled that of the antecedent seasons. The results for the Tibetan Plateau are consistent with their finding. In addition, the standard deviation of the spatial distribution of precipitable water in the 680–310 hPa level shows that the area with the highest positive trend also had the maximum difference between precipitable water datas.

Water vapor in the atmosphere is the main source of moisture for precipitation and runoff on land areas by lateral transport, and precipitation is the primary channel for bringing water to the surface. Zhai and Eskridge [19] noted that although it is difficult to explain the cause and effect between precipitable water and precipitation, the correlation between them is significant. Fig. 2a using the CRU data shows the trends of precipitation over the Earth, Northern Hemisphere, and Tibetan Plateau. We found that during 1984–2009, global and Northern Hemisphere precipitation displayed a clear increasing trend of 15.35 mm per decade ($p < 0.01$) and 12.55 mm per decade ($p < 0.01$), respectively. However, over the Tibetan Plateau, annual precipitation displayed only a small increase of about 0.27 mm per decade ($p < 0.3$). Our analysis of station data confirmed this result. A small increasing trend was found for 97 in situ measurements of precipitation, but the value was less than 1 mm per decade.

A drought index usually measures the departure from the local normal conditions and is a moisture variable based on its historical distributions [20]. Fig. 2c shows the spatial distribution of the PDSI trend over the Tibetan

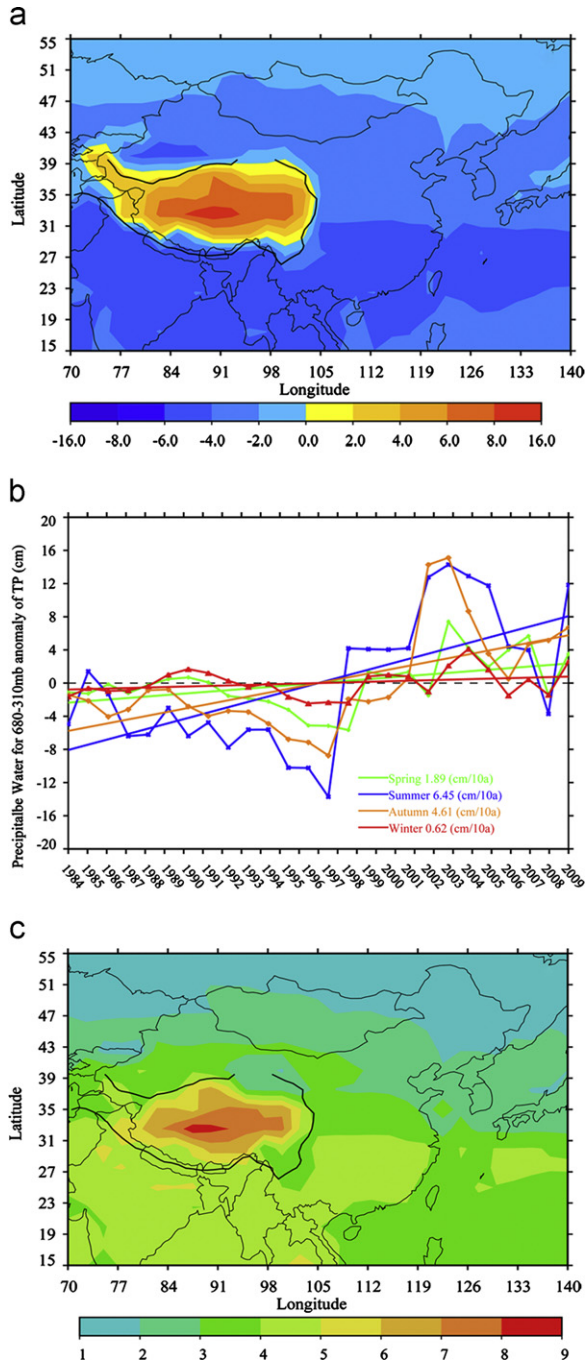


Fig. 1. Spatial distribution of the trend of precipitable water at 680–310 hPa during 1984–2009 (a). The linear trend of precipitable water at 680–310 hPa during 1984–2009 (b). Spatial distribution of the standard deviation of precipitable water in 680–310 hPa during 1984–2009 (c) over the Tibetan Plateau.

Plateau. If the value is between -1 and 1 , there was no distinct wetting or drying change in the region. If the value is greater than 1 , the surface became wetter. If the value is less than -1 , the surface became drier. This graph shows that over the southern region, along the Himalaya Mountain areas of the Tibetan Plateau, there were

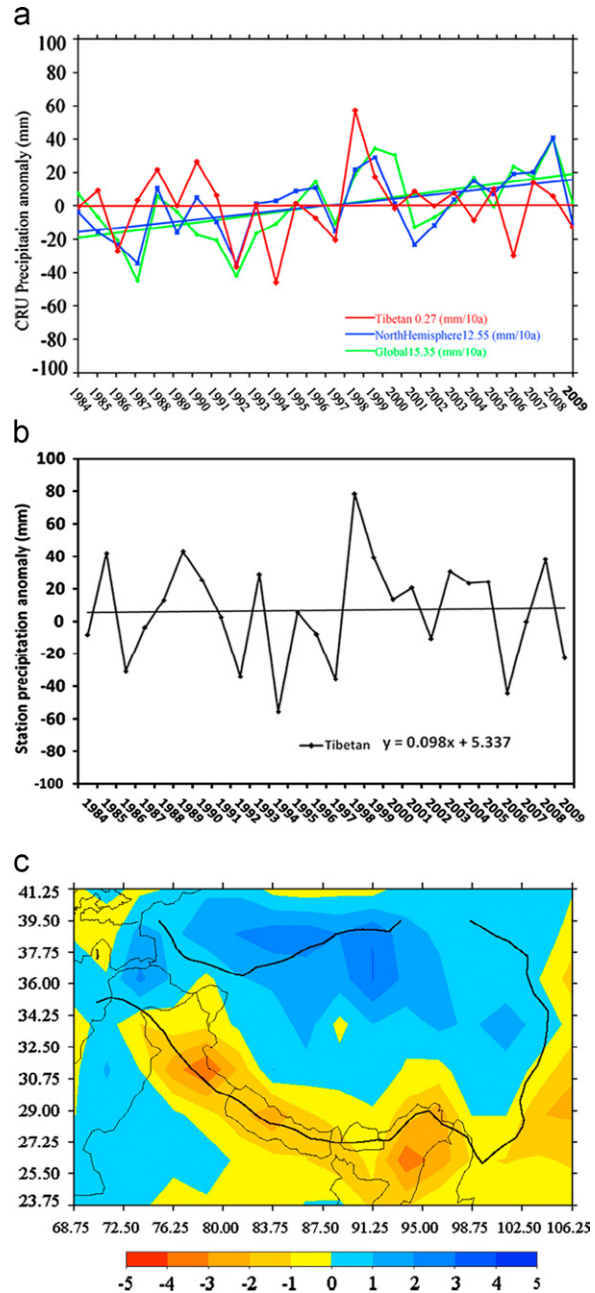


Fig. 2. Linear trend of precipitation over the Tibetan Plateau, Northern Hemisphere, and global during 1984–2009 by CRU data (a). The linear trend of precipitation over the Tibetan Plateau from the surface station data (b) and the spatial distribution of the trend of PDSI over the Tibetan Plateau (c).

decreasing trends of PDSI with a -5 per decade minimum value ($p < 0.05$). The northern region of the Tibetan Plateau exhibited increasing trends, and the center region of the Tibetan Plateau displayed no significant change in the period of 1984–2009.

Because of the location of the Tibetan Plateau and the scope of the South Asian monsoon, the low-latitude oceans are one of the main sources of water vapor for the plateau. Wu and Zhang [21] found that the Tibetan

Plateau acts as a strong “dynamic pump” that continuously attracts moist air from the low-latitude oceans in summer. During winter, a persistent anticyclone that occurs over the Arabian Sea, along the coast of Somalia, transports water vapor via the westerly jet into the plateau region. In addition to the ocean, the Tibetan Plateau itself is another major source of water. Stored water on the plateau enters the water cycle and moves into the atmosphere.

Fig. 3 shows the trend of South Asian summer monsoon index (SASMI) during 1948–2010. The SASMI is defined as an area-averaged seasonal (June, July, August, September: JJAS) dynamical normalized seasonality (DNS) at 850 hPa within the South Asian domain (5–22.5°N, 35–97.5°E) [22–24]. The South Asian summer monsoon

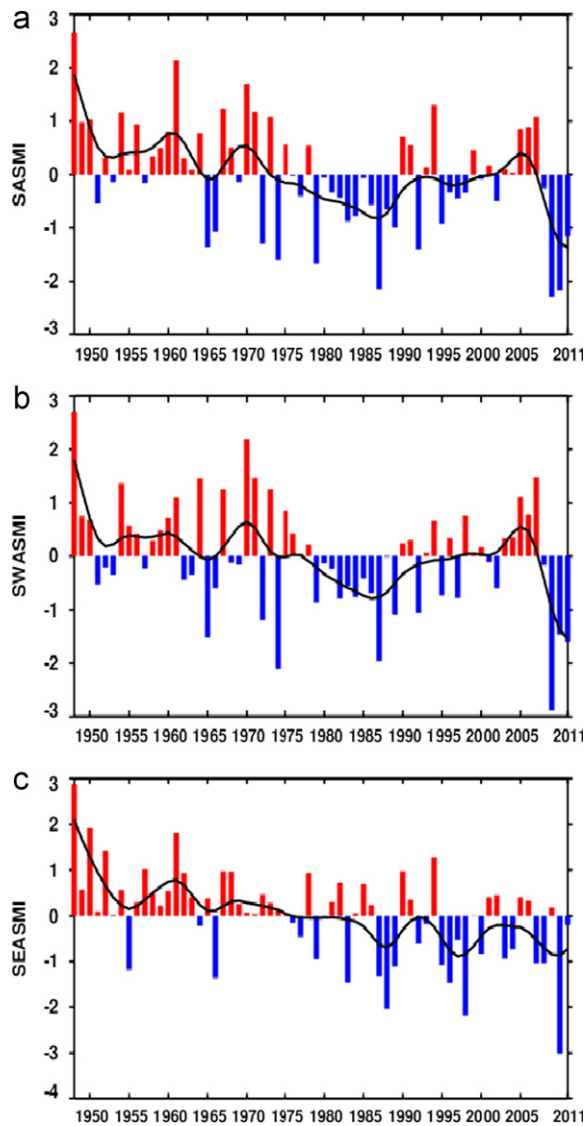


Fig. 3. Normalized time series of the SASMI (a), SWASMI (b) and SEASMI (c) during 1948–2010. The summer here is June, July, August, and September. The thick solid lines indicate 9-year Gaussian-type filtered values.

(SASM) contains two independent components, the Southwest Asian summer monsoon (SWASM) over Southwest Asia (2.5–20°N, 35–70°E) and the Southeast Asian summer monsoon (SEASM) over Southeast Asia (2.5–20°N, 70–110°E), with quite different dynamical influences on monsoon rainfall over South Asia [22,25]. The summer monsoon indices over Southwest and Southeast Asia are abbreviated SWASMI and SEASMI, respectively. SASMI and SWASMI display a similar tendency in Fig. 3, with a long-term decreasing trend from the 1950s to 1980s, then a weak increasing trend since the mid-1980s, and a sharp decreasing trend in recent years. Fig. 3 also shows a decadal change in the mid-1970s, with the strong South Asian summer monsoon phase transferring to a weak summer monsoon phase. According to the period of precipitable water (1984–2009), the South Asian monsoon is in a weak summer monsoon phase. Although the ability of transferring water vapor to be transferred will be weakened compared to the strong monsoon phase, the transmission of total water vapor is increasing year by year. This suggests that the water vapor supplied from the low-latitude oceans is one reason for the enhanced precipitable water over the Tibetan Plateau in summer from 1984 to 2009. Using a multi-model ensemble simulation, Zhang and Guo [26] found an intensification in winter of the East Asian subtropical westerly jet intensity and a northward migration of the jet axis compared with 20th century simulation results. Cai et al. [27] further confirmed that the enhancement of the jet was enhanced since the 1980s by comparing modeling results with National Centers for Environmental Prediction/National Center for Atmospheric Research (NCEP/NCAR) reanalysis data. Several recent studies [28–32] have also estimated that during the twenty-first century, global warming will shift the boundaries of the Hadley circulation and subtropical dry zone poleward. The subtropical jet is located at the poleward boundaries of the Hadley cell, and thus the subtropical jet would also move poleward under global warming. The enhancement of the intensity of the subtropical jet and its poleward movement would further affect the transport of water from the Arabian Sea to the Tibetan Plateau region. This would probably allow more water vapor to reach the plateau. Because precipitation is much higher in summer, the contribution of the enhanced precipitation is also larger in summer than in other seasons. Overall, whether in summer or winter, the transport of water vapor made a positive contribution to the increase in precipitable water vapor over the plateau during the period of 1984–2009. Another possible mechanism for the increased water vapor over the Tibetan Plateau may be the increase in surface air temperature over the Tibetan Plateau, which would allow the air above the plateau to hold more moisture. Observations indicate that the average global surface temperature has increased by 0.2–0.3 °C over the last 40 years and the increase has accelerated since the 1980s. However, the warming has not been uniform across the global [33]. There are large regional differences in the change in surface air temperature [33], and many studies have shown a relationship between surface temperature changes and elevation [34]. The mean elevation of the Tibetan Plateau is more than

4000 m a.s.l. We found that significant warming has occurred over the Tibetan Plateau since the 1980s, and this warming is larger than that in other regions. Fig. 4a shows the temperature variation from 1984 to 2009 over the Tibetan Plateau, Northern Hemisphere land surfaces, and the globe. The warming trend of temperature over the Tibetan Plateau is $0.46\text{ }^{\circ}\text{C}$ per decade ($p < 0.01$), which is greater than the increases in the Northern Hemisphere ($0.38\text{ }^{\circ}\text{C}$ per decade, $p < 0.01$), and for the globe ($0.32\text{ }^{\circ}\text{C}$ per decade, $p < 0.01$) and approximately 1.5 times the overall rate of global warming. Among the seasons, the winter temperature trend in the Tibetan Plateau, with a maximum value of $0.53\text{ }^{\circ}\text{C}$ per decade ($p < 0.01$), is the most pronounced. The winter temperature anomaly also has the largest variability, but it displays weak trends in spring (enhanced warming over the Tibetan Plateau) and summer ($0.33\text{ }^{\circ}\text{C}$ per decade, $p < 0.01$). The enhanced warming over the Tibetan Plateau is also shown in Fig. 4b, which presents the temperature trend at 97 meteorological stations across the Tibetan Plateau. This rate of warming has reached $0.67\text{ }^{\circ}\text{C}$ per decade ($p < 0.01$) and demonstrates a clear accelerated rate of warming over the Tibetan Plateau.

The accelerated warming over the Tibetan Plateau has directly affected its snow, glaciers, and permafrost. In the past half-century, 82% of the plateau's glaciers have

retreated. In the past decade, 10% of its permafrost has degraded [35]. The Tibetan Plateau is the largest glaciated area in the low to mid-latitudes in the world. Its glaciers cover about $47,000\text{ km}^2$, mainly in the Kunlun, Himalaya, and Karakorum mountains, which contain more than half of the total number and volume of glaciers on the Tibetan Plateau [36]. Many studies have shown strong evidence of an increase in the rate of glacier retreat across the Tibetan Plateau since the 1980s [37] and that the retreat is still continuing. In the Himalaya, for example, the glacier area was found to have decreased by 21% from 2077 km^2 in 1962 to 1628 km^2 in 2001–2004 [38]. In the past decade, most glaciers in the region have also shown a declining trend in albedo in their upper areas, indicating that they have generally become darker [39]. From Fig. 2c, we can see that the drier area, as indicated by the PDSI, is only the Himalayas, the location of the largest alpine glaciers and one of the most severe glacier retreat areas.

Snow over the plateau is also decreasing. Fig. 5a shows the trend of snow depth over the Tibetan Plateau. The data used here are based on passive microwave satellite observations and were combined with long-term historical in situ measurements. The figure shows an increasing trend of snow depth over the Tibetan Plateau in the 1980s, with an increase of 0.496 cm per decade ($p < 0.01$). However, this became a decreasing trend that reached -0.082 cm per decade ($p < 0.05$) during 1987–2008 and further decreased to -0.1 cm per decade ($p < 0.05$) in 2002–2010. The melting of snow has clearly accelerated. Fig. 5b shows the snow cover trend in spring and winter during the period of 2000–2011. We found that the decrease ($p < 0.01$) in snow cover over the Tibetan Plateau has been continuing, especially in recent years. Most investigations that have used in situ measurements have also shown a decreasing trend since the 1980s, in contrast to the increasing trend before the 1970s [40–43], which is consistent with our results over the plateau. The winter warming on the Tibetan Plateau has been most pronounced, in agreement with previous reports. For example, Peng et al. [44] found that mean winter snow depth values over the Tibetan Plateau were generally $< 3\text{ cm}$ and that maximum winter snow depth and mean winter snow depth at almost all Tibetan stations displayed declining trends from 1980 to 2005.

Fig. 5c shows the distribution of the evaporation trend over the Tibetan Plateau during 1984–2009, based on data from 78 weather stations. It suggests that pan evaporation decreased at most stations, with the maximum value reaching -40.39 mm per decade. This declining trend in pan evaporation is contrary to the expected effect of global warming. Two hypotheses have been proposed to explain this contradiction. First is the complementary relationship hypothesis proposed by Bouchet [45], which involves a feedback mechanism between actual evaporation and potential evaporation for homogeneous surfaces with low heat and moisture advection. This hypothesis suggests that a decrease in potential evaporation will result in an increase in actual evaporation. The second hypothesis is that a decrease in solar radiation or an increase in cloud cover plays a major role in the decrease of pan evaporation. In general, pan evaporation is a

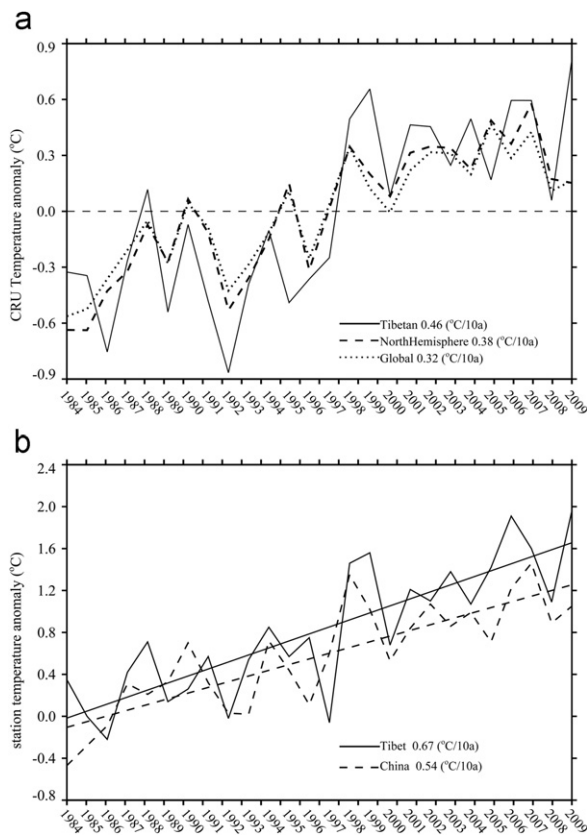


Fig. 4. Trend of temperature over the Tibetan Plateau, Northern Hemisphere, and global during 1984–2009 from CRU data (a) and the trend of temperature over the Tibetan Plateau and China from the surface station data (b).

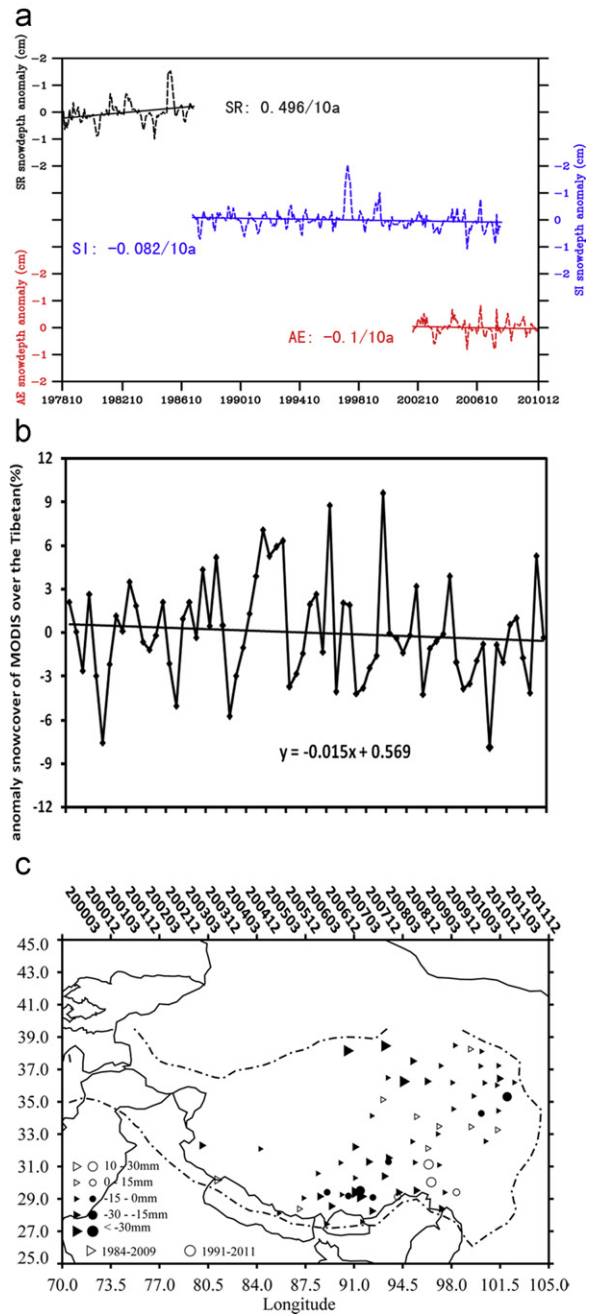


Fig. 5. Linear trend of snow depth during 1978–2010 from retrieval data based on passive microwave satellite observations (a). The labels “SR” “SI” and “AE” stand for SMMR, SSM/I, and AMSR-E, respectively. The linear trend of snow cover in winter and spring during 2000–2011 by the MODIS/Terra data (b). The spatial distribution for the trend of evaporation during 1984–2009 by the station data (c).

surrogate of potential evaporation. Recent studies [46,47] have indicated that potential (or pan evaporation) and actual evapotranspiration depend on each other in a complementary manner in the Tibetan Plateau region. Bouchet’s complementary hypothesis is not supported in the present study, possibly because of the very low vapor pressure deficit. Our results essentially imply an

increasing trend of actual evaporation over the Tibetan Plateau from 1984 to 2009. This suggests that the accelerated melting of glaciers and snow may provide another source of the increasing precipitable water in the region.

4. Discussion

Precipitable water in the higher layers has increased since the 1990s, but precipitation has displayed only a small increasing trend. At the same time, the land surface has not become wetter but has instead become drier along the Himalaya mountain areas. All of these results suggest that the increased water vapor in the atmosphere did not result in greater water resources on the plateau. On the contrary, the original storage of water resources in the Himalayas has been reduced, with water resources being lost to the atmosphere over the Tibetan Plateau. In addition, the results indicate that after the 1980s precipitation was no longer the dominant driver of changes in the terrestrial water budget. Other factors, such as surface warming, cloud-induced changes in solar radiation, and change in other fields (i.e., wind speed and humidity) have also become important.

Fig. 6a shows the trend of total cloud cover over the Tibetan Plateau. Total cloud cover decreased during 1984–2009 with a trend of -1.56% per decade ($p < 0.05$). Fig. 6b shows that dust storm activity over most regions of the

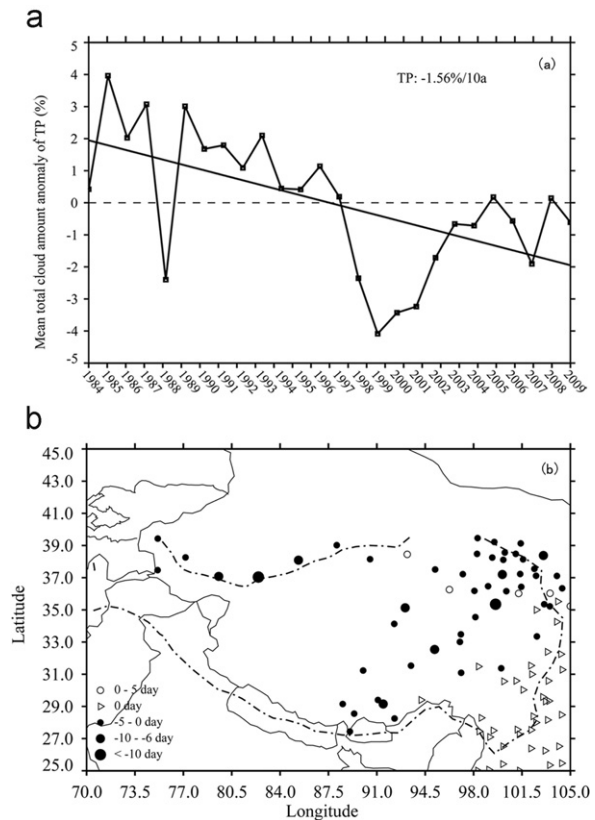


Fig. 6. Trend of total cloud cover over the Tibetan Plateau during 1984–2009 (a) and the trend of dust storm over the Tibetan Plateau during 1984–2009 (b).

plateau exhibited a decreasing trend. Huang et al. [48] found that dust plumes are transported over western Tibet from the northern part of the Taklimakan Desert. The dust aerosols act as cloud condensation nuclei, which are important for the processes of precipitation. Dust aerosols have not only a direct influence on cloud development, but also a direct influence on precipitation [49–51]. Mineral dust in the atmosphere and its effects on clouds and precipitation can have a substantial impact on regional climate [52,53]. Fig. 6a and b suggests that the decreasing trend of dust storm activity is one reason for the decreasing total cloud cover and might also be linked to the loss of water resources in the air over the Tibetan Plateau. Dust aerosols influence cloud cover and precipitation over the Tibetan plateau, but further research is needed to clarify the strength of dust effects.

5. Summary

This study found a maximum long-term positive trend of atmospheric water vapor over the Tibetan Plateau at 680–310 hPa during 1984–2009. This trend is distinct from that in surrounding areas, and the highest positive trend was found over the central plateau region. The increasing moisture in the atmosphere over the Tibetan Plateau mainly arises from two sources. The first is the rapid glacier and snow melting on the Tibetan Plateau under recent global warming conditions. The other source of increasing precipitable vapor is regional transport. In summer, this arises from low-latitude ocean sources as a result of the weaker increased South Asian summer monsoon, and in winter it comes from the Arabian Sea following the intensification of the northward movement of the subtropical jet. Although the precipitable water at higher layers has increased, it has not resulted in greater water resources on the plateau. The accelerated warming over the Tibetan Plateau has directly affected its snow and glaciers. Precipitation displayed a small increasing trend but because actual evaporation also displayed an enhanced trend due to global warming and thus the environment of the Tibetan Plateau has not become more humid. The region has actually become drier, especially in areas along the Himalaya Mountains, with water resources over the Tibetan Plateau also being lost annually. If there are no changes in other factors (such as enhanced global warming) and the monsoonal circulation does not transfer to the strong phase, the loss of water from this important Asian water tower will continue to accelerate, and the water supplies of billions of people will be at risk.

Acknowledgments

This research was supported by the National Basic Research Program of China (2012CB955301). We are grateful for the ISCCP data, which were obtained from the NASA Langley Research Center Atmospheric Sciences Data Center, the CRU data from the Climate Research Unit, the in situ measurements data from the China Meteorological Data Sharing Service System, the long-term snow depth dataset from the Environmental and Ecological Science Data Center for West China National

Natural Science Foundation of China, and the snow cover data from the US National Snow and Ice Data Center. We would like to express appreciation to Dr. Dai (<http://www.cgd.ucar.edu/cas/adai/data-dai.html>) and Dr. Li (<http://ljp.lasg.ac.cn/dct/page/65576>), for providing the PDSI data and SAMI data used in this study.

References

- [1] Ding YH. The outlook of environmental changes in western China. In: Ding YH, editor. Assessment of environment evolution of Western China, Beijing: Science; 2002. [p. 147–170 Chinese].
- [2] Lu CX, Yu G, Xie GD. Tibetan Plateau serves as a water tower. IEEE Trans Geosci Remote Sensing 2005;5:3120–3.
- [3] Lau WKM, Kim MK, Kim KM, Lee WS. Enhanced surface warming and accelerated snow melt in the Himalayas and Tibetan Plateau induced by absorbing aerosols. Environ Res Lett 2010;5:025204. <http://dx.doi.org/10.1088/1748-9326/5/2/025204>.
- [4] Xu XD, Lu CG, Shi XH, Gao ST. World water tower: an atmospheric perspective. Geophys Res Lett 2008;35:L20815. <http://dx.doi.org/10.1029/2008GL035867>.
- [5] Trenberth KE, Fasullo J, Smith L. Trends and variability in column-integrated atmospheric water vapor. Climate Dyn 2005;24:741–58.
- [6] Rossow WB, Walker AW, Beusichel DE, Roiter MD. International Satellite Cloud Climatology Project (ISCCP) documentation of new cloud datasets. WMO/TD-no. 737. World Meteorological Organization; 1996. Available from: <<http://isccp.giss.nasa.gov/docs/documents.html>>.
- [7] Che T. China deep snow time series data set (1978–2010). Cold and Arid Regions Environmental and Engineering Research Institute. Chinese Academy of Sciences; 2012. Available from: <<http://westdc.westgis.ac.cn/data/f957004d-0756-4796-b4c5-c02265be64e1>>.
- [8] Che T, Li X, Jin R, Armstrong R, Zhang TJ. Snow depth derived from passive microwave remote-sensing data in China. Ann Glaciol 2008;49:145–54.
- [9] Dai LY, Che T. Cross-platform calibration of SMMR, SMM/I and AMSR-E passive microwave brightness temperature. Sixth international symposium on digital earth: data procession and applications. In: Guo HD, Wang CL, editors. Proceedings of SPIE; 2010. 78412010.
- [10] Hall DK, George AR, Salomonson VV. MODIS/Terra snow cover monthly L3 global 0.05deg CMG V005. (2000.03–2012.03). Boulder, Colorado, USA: National Snow and Ice Data Center, Digital media 2006. Available from: <http://nsidc.org/data/docs/daac/modis_v5/mod10cm_modis_terra_snow_monthly_global_0.05deg_cmg.gd.html>.
- [11] Hall DK, Foster JL, Salomonson VV, Klein AG, Chien JYL. Development of technique to assess snow cover mapping errors from space. IEEE Trans Geosci Remote Sensing 2001;39:432–8.
- [12] Riggs GA, Hall DK, Salomonson VV. MODIS sea ice products user guide, February 2003. Available from: <<http://modis-snow-ice.gsfc.nasa.gov/siugkc.html>>.
- [13] Pu ZX, Xu L, Salomonson VV. MODIS/Terra observed seasonal variations of snow cover over the Tibetan Plateau. Geophys Res Lett 2007;34:L06706. <http://dx.doi.org/10.1029/2007GL029262>.
- [14] Mitchell TD, Jones PD. An improved method of constructing a database of monthly climate observations and associated high-resolution grids. Int J Climatol 2005;25:693–712.
- [15] Dai AG, Trenberth KE, Qian TT. A global dataset of palmer drought severity index for 1870–2002: relationship with soil moisture and effects of surface warming. J Hydrometeorol 2004;5:1117–30.
- [16] Li JP. Institute of Atmospheric Physics, Chinese Academy of Sciences. Available from: <<http://ljp.lasg.ac.cn/dct/page/65576>>.
- [17] Climatic Research Unit (CRU). University of East Anglia. Available from: <<http://www.cru.uea.ac.uk/cru/data/temperature/>>.
- [18] Peixoto JP, Salstein DA, Rosen RD. Intra-annual variation in large-scale moisture fields. J Geophys Res 1981;86:1255–64.
- [19] Zhai P, Eskridge RE. Atmospheric water vapor over China. J Climate 1997;10:2643–52.
- [20] Dai AG. Drought under global warming: a review. WIREs Climate Change 2011;2:46–65. <http://dx.doi.org/10.1002/wcc.81>.
- [21] Wu GX, Zhang YS. Tibetan Plateau forcing and the Asian monsoon onset over South Asia and South China Sea. Mon Weather Rev 1998;126:913–27.
- [22] Li JP, Zeng QC. A unified monsoon index. Geophys Res Lett 2002;29(8):1151–4. <http://dx.doi.org/10.1029/2001GL013874>.

- [23] Li JP, Zeng QC. A new monsoon index and the geographical distribution of the global monsoons. *Adv Atmos Sci* 2003;20: 299–302.
- [24] Li JP, Zeng QC. A new monsoon index, its inter-annual variability and relation with monsoon precipitation. *Climatic Environ Res* 2005;10(3):351–65.
- [25] Wang B, Fan Z. Choice of South Asian summer monsoon indices. *Bull Am Meteorol Soc* 1999;80:629–38.
- [26] Zhang YC, Guo LL. Multi-model ensemble simulated changes in the subtropical westerly jet over East Asia under the global warming condition. *Sci Meteorol Sin* 2010;30(5):694–700.
- [27] Cai QQ, Zhou TJ, Wu B, Li B, Zhang LX. The East Asian subtropical westerly jet and its interannual variability simulated by a climate system model FGOALS_g1. *Acta Oceanol Sin* 2011;33(4):38–48.
- [28] Seidel DJ, Fu Q, Randel WJ, Reichler TJ. Widening of the tropical belt in a changing climate. *Nat Geosci* 2008;1:21–4.
- [29] Williams GP. Circulation sensitivity to tropopause height. *J Atmos Sci* 2006;63:1954–61.
- [30] Lorenz DJ, DeWeaver ET. Tropopause height and zonal wind response to global warming in the IPCC scenario integrations. *J Geophys Res* 2007;112:D10119.
- [31] Polvani LM, Kushner PJ. Tropospheric response to stratospheric perturbations in a relatively simple general circulation model. *Geophys Res Lett* 2002;29(7):1114. <http://dx.doi.org/10.1029/2001GL014284>.
- [32] Haigh JD, Blackburn M, Day R. The response of tropospheric circulation to perturbations in lower-stratospheric temperature. *J Climate* 2005;18:3672–85.
- [33] Huang JP, Guan XD, Ji F. Enhanced cold-season warming in semi-arid regions. *Atmos Chem Phys* 2012;12:5391–8.
- [34] Liu XD, Chen BD. Climatic warming in the Tibetan Plateau during recent decades. *Int J Climatol* 2000;20:1729–42.
- [35] Qiu J. China: the third pole. *Nature news feature*, July 24 2008; 454:393–6. [10.1038/454393a](http://dx.doi.org/10.1038/454393a).
- [36] Liu ZX, Su Z, Yao TD, Wang WT, Shao WZ. Resources and distribution of glaciers on the Tibetan Plateau. *Resour Sci* 2000;22(5): 49–52 [Chinese].
- [37] Pu JC, Yao TD, Wang NL, Su Z, Shen YP. Fluctuations of the glaciers on the Qinghai Tibetan Plateau during the past century. *J Glaciol Geocryol* 2004;26(5):517–22 [Chinese].
- [38] Kulkarni AV, Bahuguna IM, Rathore BP, Singh SK, Randhawa SS, Sood RK, et al. Glacial retreat in Himalaya using Indian remote sensing satellite data. *Curr Sci* 2007;92(1):69–74.
- [39] Ming J, Du ZC, Xiao CD, Xu XB, Zhang DQ. Darkening of the mid-Himalaya glaciers since 2000 and the potential causes. *Environ Res Lett* 2012;7:014021. <http://dx.doi.org/10.1088/1748-9326/7/1/014021>.
- [40] Zhang YS, Li T, Wang B. Decadal change of the spring snow depth over the Tibetan Plateau: the associated circulation and influence on the East Asian summer monsoon. *J Climate* 2004;17:2780–93.
- [41] Qin DH, Liu SY, Li PJ. Snow cover distribution, variability, and response to climate change in western China. *J Climate* 2006;19: 1820–33.
- [42] Yang JP, Ding YJ, Liu JF. Distribution of snow cover and its inter-decadal variation in the source regions of the Yangtze and Yellow rivers. *J Glaciol Geocryol* 2006;28(5):648–55 [Chinese].
- [43] Pu ZX, Xu L. MODIS/Terra observed snow cover over the Tibet Plateau: distribution, variation and possible connection with the East Asian Summer Monsoon (EASM). *Theor Appl Climatol* 2009;97:265–78. <http://dx.doi.org/10.1007/s00704-008-0074-9>.
- [44] Peng SS, Piao SL, Ciais P, Fang JY, Wang XH. Change in winter snow depth and its impacts on vegetation in China. *Global Change Biol* 2010;16:3004–13. <http://dx.doi.org/10.1111/j.1365-2486.2010.02210.x>.
- [45] Bouchet RJ. Evapotranspiration réelle et potentielle, signification climatique. Paper presented at Symposium, Publ. 62. Berkeley CA: International Association of Scientific Hydrology. p. 134–42.
- [46] Zhang YQ, Liu CM, Tang YH, Yang YH. Trends in pan evaporation and reference and actual evapotranspiration across the Tibetan Plateau. *J Geophys Res* 2007;112:D12110. <http://dx.doi.org/10.1029/2006JD008161>.
- [47] Yang K, Ye BS, Zhou DG, Wu BY, Thomas F, Qin J, et al. Response of hydrological cycle to recent climate changes in the Tibetan Plateau. *Climate Change* 2011;109:517–34. <http://dx.doi.org/10.1007/s10584-011-0099-4>.
- [48] Huang JP, Minnis P, Yi YH, Tang Q, Wang X, Hu YX, et al. Summer dust aerosols detected from CALIPSO over the Tibetan Plateau. *Geophys Res Lett* 2007;34:L18805. <http://dx.doi.org/10.1029/2007GL029938>.
- [49] Huang JP, Minnis P, Lin B, Wang TH, Yi YH, Hu YX, et al. Possible influences of Asian dust aerosols on cloud properties and radiative forcing observed from MODIS and CERES. *Geophys Res Lett* 2006;33:L06824. <http://dx.doi.org/10.1029/2005GL024724>.
- [50] Huang JP, Lin B, Minnis P, Wang TH, Wang X, Hu YX, et al. Satellite-based assessment of possible dust aerosols semi-direct effect on cloud water path over East Asia. *Geophys Res Lett* 2006;33: L19802. <http://dx.doi.org/10.1029/2006GL026561>.
- [51] Huang JP, Fu Q, Su J, Tang Q, Minnis P, Hu Y, et al. Taklimakan dust aerosol radiative heating derived from CALIPSO observations using the Fu–Liou radiation model with CERES constraints. *Atmos Chem Phys* 2009;9:4011–21.
- [52] Li ZQ, Li C, Chen H, Tsay C, Holben B, Huang JP, et al. East Asian Studies of tropospheric aerosols and their impact on regional climate (EAST-AIRC): an overview. *J Geophys Res* 2011;116: D00K34. <http://dx.doi.org/10.1029/2010JD015257>.
- [53] Wang X, Huang JP, Ji MX, Higuchi K. Variability of East Asia dust events and their long-term trend. *Atmos Environ* 2008;42: 3156–65.